JOURNAL OF APPLIED POLYMER SCIENCE VOL. 14, PP. 1143–1158 (1970)

Predicting Joint Sealant Performance of Elastomers by Computer Simulation. I. Justification of Method

E. H. CATSIFF, R. F. HOFFMAN, and R. T. KOWALEWSKI, *Thiokol Chemical Corporation, Chemical Division, Trenton, N. J. 08607*

Synopsis

A computerized method has been developed for the analysis of the behavior of a sealed joint. The method is based upon the use of fundamental time-dependent mechanical properties of a polymeric sealant, which can be easily determined in the laboratory, to feed a digital computer program that performs internal force balances within a given joint seal configuration by dividing the joint seal into a large number of "finite elements" in which the sealant properties are invariant. The computational method is an outgrowth of stress analysis programs that have been developed for use in the study of stress distributions within solid rocket propellant "grains." Output from the computer program consists of a prediction of the overall geometric deformation of the sealant and the distribution of stresses and strains within the joint seal. Essential to the ideologic development of this method is the "separability" of time-dependent and strain-dependent aspects of the behavior of the material properties. However, the method should be operable even when this "separability" is only approximately maintained, as in many real materials. Fundamental properties have been determined on several typical sealant materials. A description is given of the mode of operation of the computational method, but detailed results are given in a companion article.

INTRODUCTION

The sealing of joints between essentially rigid components of various structures is a vital (to the structure) yet not well known application of many types of polymeric or quasipolymeric materials. For example, the expansion joints of a concrete roadway, the gap between glass window and wooden or aluminum window frame, and the seams of a flush-jointed boat all require a sealant to curb the passage of air, water, heat, etc. Traditional inexpensive sealant materials (putty, tar, and the like) are widely used, but in joints where the rigid members undergo significant movement relative to each other (so-called "dynamic" joints), a considerable degree of elastomer-like material behavior is needed. The variety of types of joint configurations that need to be sealed is limited only by the imagination of the designers and devisers of the structures; the movements that may occur during and after construction are even more varied. Most structures are exposed to a fairly broad range of temperatures, and it is notorious that elastomeric materials undergo marked changes in behavioral properties precisely in the temperature ranges that are of concern to structural planners. A typical situation is the widening of a gap between sections of a building wall because of thermal contraction in cold weather, combined with an increase in stiffness and brittleness of the gap-sealant material at these same temperatures. In consequence of this multiplicity of end-use requirements, it is essentially impossible to develop a universal set of sealant specifications. Instead, it has usually been necessary to develop specifications for each individual use and to modify the specifications empirically when shortcomings appear.[1]

Since a joint sealant must perform a mechanical function, specification of its mechanical behavior is logical. (Other considerations often may limit the possible choice of materials; e.g., the sealant material must not adversely affect the substrate to which it is applied, nor may the substrate or the environment adversely affect the sealant's properties.) Several general-purpose mechanical tests are widely used as specifications: tensile breaking stress and strain, "rubber modulus" at various elongations, compression set or stress relaxation, and fatigue life in the Bostik Mastic Tester, have all been relied on. Relevance of the measurements obtained to actual use is likely to require an almost intuitive appreciation of past experience. Special-purpose tests may be devised, but the multiplicity of end-use requirements can be expected to yield an equal multiplicity of such tests. In any case, correlation of field failures or successes with numerous laboratory tests and controlled field tests is bound to be a tedious and time-consuming operation.

The ability to predict the performance of a given sealant material in a proposed application would be an invaluable tool in the specification of sealants and in the design of joint configurations to make optimum use of sealants. Because of the complexity of joint configurations and movements and the limitations of the simple analytical tools available, relatively few attempts have been made to predict sealant behavior in a sealed joint by theoretical means. One such attempt,[2] which concentrated on the effect of joint thickness (probably the most important single geometric factor in a butt joint), required that the shape of the deformed sealant surface be arbitrarily assumed (it was taken to be parabolic) and was limited to simple rectangular butt joints. The distribution of stress and strain was also arbitrarily assumed to follow a certain simple pattern. Subsequent work[3] has also been based on this particular group of assumptions. On the other hand, true fundamental analysis requires not only that the geometric complexity of the real joint should be allowed, but that the nonlinearly viscoelastic properties of the sealant material should be considered as well.

We have approached this problem from the standpoint of applying a continuum mechanical model which exhibits the fundamental viscoelastic material properties of a given sealant substance. The determination of the fundamental properties may be done in a geometrically simple situation. These properties may then be applied to the continuum model by a computer program which permits the needed geometric and viscoelastic complexity. Not only overall material deformation but also stress and strain distributions may be predicted under various loading conditions. Validation of the method may be sought by comparison with easily measured cases (which are yet too complex for simple analysis).

If this approach proves successful, a considerable reduction may be possible in the amount of testing prior to sealant specification. Material parameters may be determined under controlled laboratory conditions, with a variety of geometric cases being accounted for after determining one set of parameters. Joint configuration and loading can be varied in the computer program to predict field performance. The influence of temperature changes, aging, and composition changes may be determined in the laboratory and used to predict field performance of the changed sealant material. If the fundamental parameters show smooth trends with these changes, interpolation and extrapolation to other cases will be greatly facilitated.

The work reported in this and the following article[4] is intended primarily to show the feasibility of the technique. Already existing computer programs were applied without essential modification; the materials testing was restricted to room temperature and only unaged materials were used. Simple extension and compression butt joints were used, with one excursion into a cycled joint.

Obviously a more sophisticated model (and considerable experimental comparisons) would be needed to consider all possible variations in joint movement, temperature cycling, joint design, and aging. Work is continuing on further applications of the model to more complex movements, cycling, and so on.

MECHANICAL PROPERTIES OF JOINT SEALANT MATERIAL

The complexity of rational analysis of joint seal behavior stems from several sources. Those which are purely geometric (i.e., the different stresses and deformations which exist simultaneously in different parts of the joint seal) will be considered in a later section. The fundamental viscoelastic properties of the sealant material also contribute complexity, since these properties are dependent on both time (after application of stress or deformation) and deformation. In the general case, both effects may interact so that the stress–strain–time description of even a simple deformation becomes exceedingly complex. Rational analysis of such materials is beyond the scope of this work.

It was pointed out by Smith,[5] citing many predecessors, that for many isotropic elastomers, the stress, both in stress relaxation at constant strain and in constant strain rate testing, could be expressed as a function of strain multiplied by a function of time, viz.,

$$\sigma(\epsilon,t) = \Phi(\epsilon)\cdot f(t). \tag{1}$$

The appropriate function of time would be the tensile stress–relaxation modulus, $E(t)$, or the constant strain rate tensile modulus, $F(t)$, which Smith showed to be related to one another by

$$E(t) = F(t)[1 + d \log F(t)/d \log t], \tag{2}$$

an equation derived from linear viscoelasticity theory. The function $\Phi(\epsilon)$ may be regarded as an empirical strain measure. At small strain, it must approach $\epsilon = \lambda - 1$, so that linear viscoelasticity theory will hold. The appropriate form for $g(\epsilon) = \Phi(\epsilon)/\epsilon$ was found to be $1/(1 + \epsilon)$ for both SBR gum vulcanizate and NBS isobutylene, the latter being analyzed both by stress relaxation data and by constant strain rate data. In general, $g(\epsilon)$ must be regarded as an empirical function to be determined for each material. Likewise, $E(t)$ or $F(t)$ is an empirical function of time which must be found for each material. For a few nonrelaxing materials, $E(t)$ is essentially constant, but for most elastomeric and quasi-elastomeric materials, $E(t)$ relaxes more or less rapidly, either to zero or to a long-time constant value. The form of $E(t)$ is usually temperature dependent; there is a well-known principle of time–temperature equivalence[6,7] which applies to many substances. This equivalence, once established, can also facilitate rational analysis. However, the work reported now was all performed at room temperature.

From this background, certain limitations appear to be inherent in the present approach. Separability or approximate separability of time and strain effects must be demonstrable. The applicability of equations like eq. (2), derived from the theory of linear viscoelasticity, cannot be assumed without test. Alternatively, it may be shown that the time–strain history of a particular geometric case is essentially the same as the history of the simplified test samples.

MEASUREMENT

To obtain meaningful elementary material properties, geometric simplicity is essential. Simple uniaxial elongation was selected. To avoid stress concentrations at grips, ring samples were mounted over pins; this also had the advantage that crosshead motion (of the Instron tester) was directly equal to sample extension. The rings were cut from thin cast sheets (typically 0.075 in. thick) of the various elastomers tested. The rings were cut so as to have a uniform rectangular cross section, with the annular thickness about 0.04 in., i.e., less than the sheet thickness; this eliminated twisting of the rings when they were extended, a serious shortcoming with flat-ring samples.[8] (The actual thickness and width of each ring were measured prior to testing.) To cut such rings, a special cutter was used.* The initial separation of the Instron grips was 1.00 in. while the ring diameters were 0.64 in. and 0.72 in. Experimentally it was found that these

* We are deeply indebted to P. E. Meiss and W. E. Seas both for the ring-cutting device and for determining the stress–strain curves of the ring and model-joint test samples.

dimensions caused negligible initial stress to be registered by the Instron gauge, yet gave force–extension curves that rose fairly sharply from the origin. Strain was calculated on a 1.00-in. gauge length, which was within 7% of the strain calculation used by Smith[5]; his expression for gauge length would give

$$L_0 = (\pi/4)(D_i + D_0) = 1.07 \text{ in.} \tag{3}$$

The crosshead speeds used and corresponding extension rates are given in Table I. When available, ten ring samples were stretched to break at each of seven crosshead speeds. (The 50 ipm speed was not always used.)

TABLE I
Testing Speeds for Ring Samples

Crosshead speed, ipm	Elongation rate, %/min
0.2	20
0.5	50
1.0	100
2.0	200
5.0	500
10.0	1000
20.0	2000
50.0	5000

TABLE II
Materials Tested

System	Polymer type	Composition	Source	Remarks
A	Polysulfide (4000 MW, low degree of crosslinking)	30 phr MT carbon black 15 phr curing paste (50% PbO_2, 45% dibutyl phthalate, 5% stearic acid)	Thiokol Chemical Corp.	Not a commercial system; oversimplified
B	Silicone	One-part, containing a black filler	General Electric Co.	Commercial sealant
C	Silicone	One-part, containing a black filler	Dow Corning Co.	Commercial sealant
D	Polysulfide	Two-part, containing MT carbon black as a filler, cure system based on PbO_2	Thiokol Chemical Corp.	Representative of recommended commercial practice, highway sealant
E	Polyurethane	Two-part, asphalt-modified	Products Research Corp.	Commercial highway sealant
F	Polysulfide (same as A)	15 phr curing paste, (same as A)	Thiokol Chemical Corp.	Unfilled system

Certain materials proved exceedingly difficult to prepare rings from, either because they were too fast-curing to level properly in the polished molds (silicone) or too soft when "cured" (commercial polyurethane–asphalt sealant and commercial polysulfide sealant). In such cases, fewer replications were, perforce, possible.

The materials tested were selected to run a gamut of sealant varieties. They included a greatly simplified polysulfide sealant containing only MT black and a PbO_2-based curing paste, two commercial silicone sealants, a commercial-type two-part polysulfide sealant, and a commercial polyurethane–asphalt two-part sealant. Table II gives a description of these materials.

Averaged stress–strain curves were obtained for all systems. It was noted that one of the silicone sealants (system C) had relatively little dependence of the stress–strain curve on the strain rate, while the other (system B) had essentially no rate dependence.

These data were intended for evaluation of the strain- and time-dependence of the shear modulus of the materials. For three-dimensional stress analysis, a second material parameter is needed to describe the behavior of isotropic materials. This, a measure of volume change or bulk modulus, is readily expressed as Poisson's ratio. For small uniaxial tensile strain, Poisson's ratio is defined as

$$\nu_0 = \epsilon_{lat}/\epsilon, \tag{4}$$

and an infinitesimal constant-volume extension is expressed by $\nu_0 = 0.5$. For finite extension, however, the relationship between volume change and ν_0 becomes more complex, and a more general definition of Poisson's ratio[17] becomes preferable, viz.,

$$\nu = 0.5(1 - \ln J_3/\ln \lambda). \tag{5}$$

The ν value reduces to ν_0 as $\lambda \rightarrow 1$, of course, but remains constant at 0.5 for any isovolumetric extension.

Tensile strips with circles drawn on them as benchmarks were chosen to determine Poisson's ratio. Under loading, these strips deform in uniaxial strain. Measurements were made of the major and minor axes of the deformed circles. The tensile strips (4 in. $\times$ $^1/_2$ in.) were cut from cast sheets, of systems A, D, and E. Strips were also prepared from unfilled cast sheets of the polysulfide and curing paste of system A (system F). The strips were elongated and the deformations of the circles were photographed with a Polaroid 100 camera equipped with a close-up lens using 3000 film; gauge distance was 9.75 in. between lens and subject. A scale was placed alongside the strip to provide a reference for absolute measurements; at times, resolution was possible to ± 0.02 in. The strips were extended to various elongations, up to 300% in some cases. No attempt was made to determine if the volume changes showed any time dependence.

Figure 1 presents the data correlated in the operational parameters of axial elongation and lateral contraction. The solid curve is a smoothed

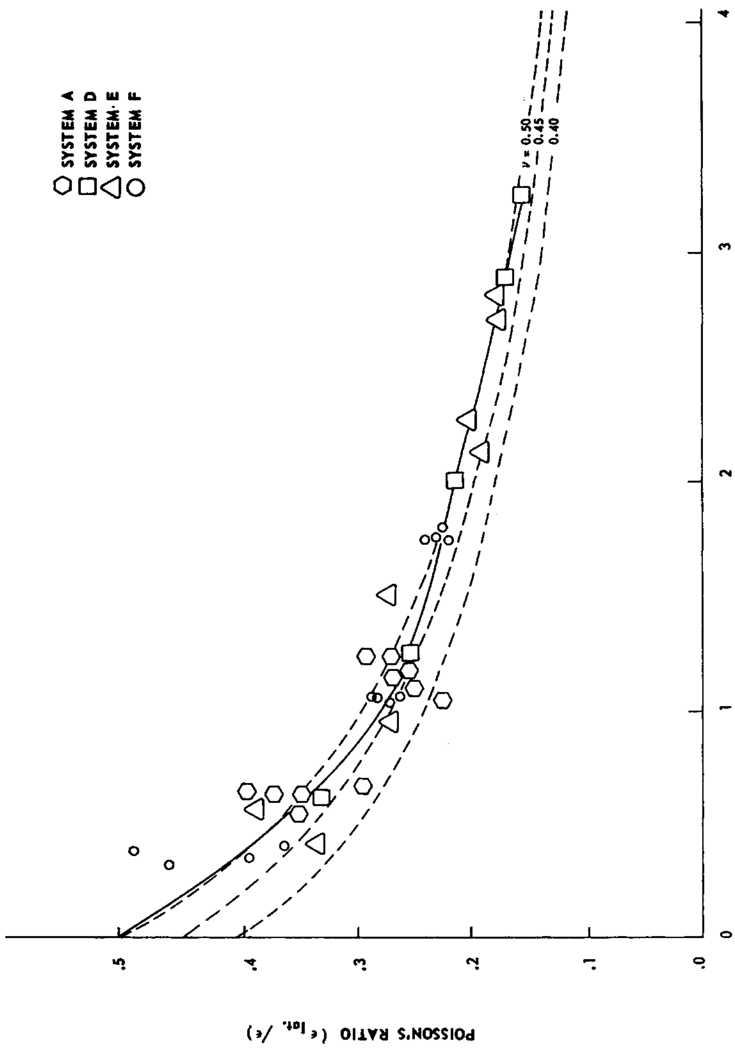

Fig. 1. Apparent value of Poisson's ratio as a function of elongation for large extensions. Systems are identified in Table II.

fit through the averages for the combined data. As would be expected, the data spread is much larger at low elongation where measurements of deformations are affected by the resolution uncertainty of ± 0.02 in.; at higher elongations, the resolution error contributions are substantially less. Overall, the curve fit is very good for the combined data, indicating that both the filled and unfilled systems behave the same way under simple tension, i.e., the introduction of filler does not disturb the Poisson ratio of the basic polysulfide system. Curves were calculated for various constant values of ν and also appear in Figure 1 as broken lines. These tend to converge at high elongations, so that the resolution error contributions to ν_0 result in a relatively larger error in ν.

From Figure 1 it was concluded that these materials all deformed at nearly constant volume. (The apparent crossover of the smoothed curve is unlikely, however.) This is essentially the behavior expected of a liquid-like continuum rubber. The resolution uncertainty (of ± 0.02 in.) translates into an uncertainty of ± 0.02 in ν.

Reduction of Data to Determine Material Property Parameters

Following Smith,[5] the constant strain rate data were replotted to facilitate determination of $F(t)$ if, indeed, it was separable from $\Phi(\epsilon)$ in eq. (1). The system A data are shown in Figure 2, plotted as log σ versus log t. Each strain rate contributed the data points shown as a curve rising toward the right. The set of parallel lines shown with negative slope represents the σ–t relationship at each constant elongation. Each of these may be regarded as a plot of $F(t)$ for its given ϵ. The Separability Eq. (1) does not require that these lines be straight, but merely that the *vertical* shifts be constant between them. The constant slope $[d \log F(t)/d \log t]$ is of great convenience in data manipulation, of course.

Since plots like Figure 2 showed that time–strain separability exists for all the systems described in Table II, isochronal stress–strain curves could be constructed by plotting σ versus ϵ values selected from Figure 2 at various constant times. Figure 3 shows selected isochrones for system A. Time effects have now been removed from the curves, so they may be regarded as plots of $\Phi(\epsilon)$ versus ϵ, and clearly display the nonlinearity of the stress–strain relationship.

This nonlinearity is the basis for many different approaches to finite elasticity theory. We have chosen to use the general approach of Herrmann et al.,[9–12] which is based on the use of the large strain tensor, E_{ij}, as defined by Green and Zerna.[13] At its present state of development, this approach sets up four strain-dependent material parameters, designated as K_1 to K_4. The first parameter was chosen so as to reduce to the shear modulus at infinitesimal strain while K_2 is related to Poisson's ratio; it is 0.5 at all deformations for a constant-volume strain. K_3 and K_4 (which are related to the strain-induced anisotropy of the material) become zero at zero strain. Proper evaluation of these latter two consequently requires an extremely elaborate and sophisticated experimental program,

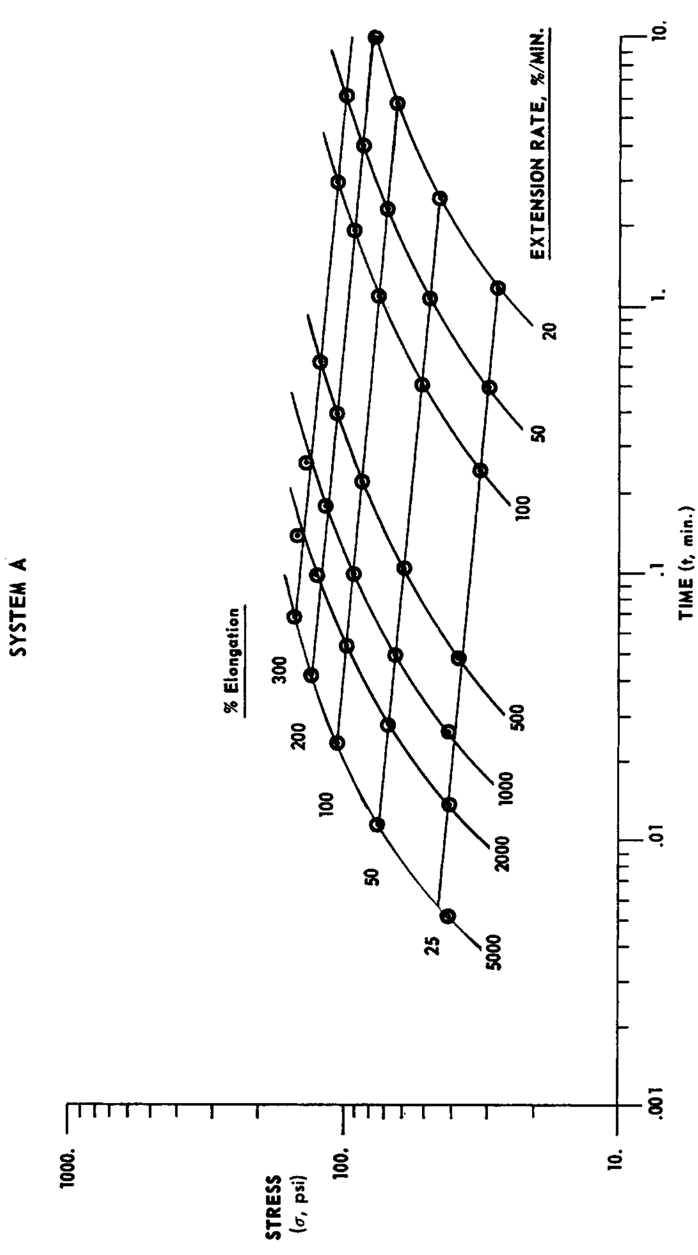

Fig. 2. Relationships of stress, strain, and time for a typical sealant composition tested at constant strain rates. System A.

such as that undertaken by Rivlin et al.,[14,15] Treloar,[16] and Blatz and Ko.[17] Since this was beyond the scope of the present feasibility demonstration, it was assumed that K_3 and K_4 retained zero values up to moderate strains. Failure of this assumption would be expected to result in failure of K_1 and

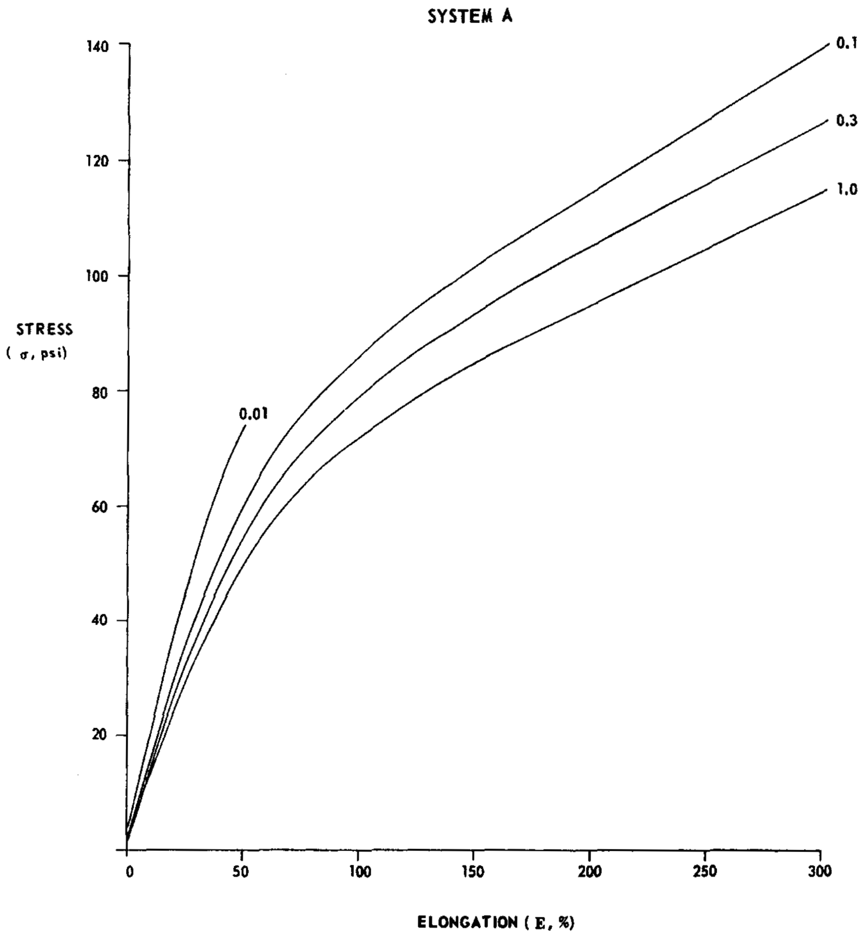

Fig. 3. Isochronous stress–strain curves derived from constant strain rate data. System A; time in minutes.

K_2 (as determined by the experimental procedures used) to predict properly the measurable stress–strain behavior of the sealant in model test joints. Since Figure 1 indicated that the systems tested all deformed at essentially constant volume, we assumed $K_2 = 0.5$ and proceeded to determine K_1 from[10]

$$K_1 = \sigma/(1 - \lambda^{-3}) \tag{6a}$$

$$(K_2 = 0.5) \tag{6b}$$

Since σ is given as a set of isochronal functions of ϵ (or λ), K_1 will also be obtained as a set of isochrones varying with λ. It is interesting to consider K_1 for a material that approximately obeys the Mooney-Rivlin stress–strain law in extension[16,18]:

$$\sigma/(\lambda - \lambda^{-2}) = 2(C_1 + C_2\lambda^{-1}) \tag{7a}$$

$$\nu = 0.5 \tag{7b}$$

By comparing eqs. (6) and (7), we can see that, for such a material,

$$K_1 = 2(C_1\lambda + C_2) \tag{8a}$$

$$K_2 = \nu = 0.5. \tag{8b}$$

The Finite-Element Method

In deforming a body of sufficient size to have a distribution of stresses and strains, one approach to rational analysis is to subdivide the body into a number of elements. Each element is assumed to be of finite size, but small enough to be regarded as undergoing linear (with respect to coordinate distance) displacements of each material point and having uniform material properties.[20] The stress–strain behavior of each element is separately considered, but continuity of displacements across element boundaries and balanced forces are required. The overall behavior is obtained by a summing process that is analogous to a numerical integration.

Even though each element is simple enough to be analyzed in three dimensions to yield a full description of stress and strain, the problem of reconciling all the contributions in three dimensions is still too great for the available computer programs. For simplification, two approaches have been used:

(1) Plane strain, in which all variable deformations are confined to two dimensions, while the strain in the third dimension may be prespecified but must be uniform and homogeneous throughout all elements; variable stresses then arise in the third dimension.

(2) Plane stress, in which all stress variation is confined to two dimensions, while the strain in the third dimension is adjusted for each element to bring about zero stress.

The physical situation most closely resembling plane stress would be the deformation of a thin sheet of material with no pressure on either side and no bending torque out of the plane of the sheet. Tensile testing of dumbbells should approach this.

For plane strain, the physical situation should call for essentially infinite length in the third dimension, so that no stress-free surface bounds the specimen perpendicular to this axis. Again no bending of this direction can occur, although a *uniform* extension or contraction can be imposed parallel to this Z-axis. The geometry of a sealed joint should begin to approach plane strain since most joints are much longer than their width or thickness and many joint motions are essentially perpendicular to the length of the joint.

The available computer programs include a group that have been developed over many years within the aerospace industry to permit rational analysis of the behavior of solid propellant "grains" (i.e., cast or fabricated masses of solid propellant), which may be bonded to a case or shell, when undergoing mechanical stress or deformation. The original programs[19] were written to permit small-strain analysis, by the finite-element procedure, of material structures of some geometric complexity but having constant values of Young's modulus and Poisson's ratio. Subsequently the programs were extended to finite deformation situations and procedures for handling time dependence were devised.[9-12*]

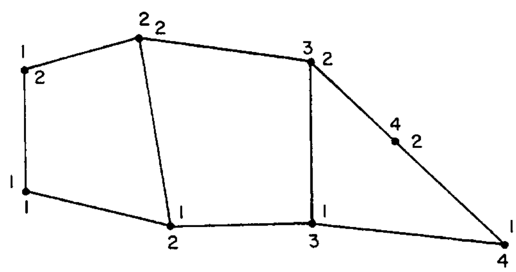

Fig. 4. Division of an arbitrary shape into three "quadrilateral" elements, one of which is actually a triangle. This is a 4 $\times$ 2 mesh.

As now constituted, the computer program imposes certain additional limits on the problems which may be undertaken. Although as many as 1000 finite elements can be handled, the calculation time (and hence the cost) goes up nearly as the square of the number of elements, so the coarsest subdivision that gives acceptable results is used. Elaborate shapes may be handled, but this requires careful attention to planning the subdivision and is likely to increase the number of elements required. Certain types of initially imposed forces and stresses are possible, but, in general, prestressed situations cannot be adequately inserted.

In operation, the program requires as input a geometric description of the specimen cross section and of its subdivision into elements. Each element must be a quadrilateral and each of the corners (nodes) must be identified by two index numbers, so that all nodes lie on a topologic two-dimensional grid. The quadrilaterals need not be geometric rectangles and may degenerate to a triangle with one node lying on the straight line between two others, but there must be four nodes and there must not be an internal angle in any element greater than 180°. (See Fig. 4 for a simple example.) The program will treat the quadrilaterals as if they were stacked

* We are also indebted to G. P. Anderson, W. A. Cook, and E. C. Dickson of the Wasatch Division of Thiokol Chem. Corp. for development of much of this program and for assistance in applying it to our problem.

in a square array (i.e., topologically two-dimensional), which also places restrictions on the type of subdivision that is acceptable. At least all of the nodes on the geometric boundary and on any internal boundaries must be fully specified, with X- and Y-coordinates given, as well as any specified restrictions, e.g., that the X-coordinate must move a certain distance (which may be zero) or that a force is specified in the Y-direction. Since several different kinds of materials can be used (this allows provision for holes or inserts in the structure), a method is provided for indicating which elements consist of each material. The properties of each material are also input, as tables of isochrones of K_1, K_2, K_3, and K_4 at selected values of E_{11}, the principal component of the large strain tensor.

For our problems we chose, as mentioned, the condition of plane strain with zero imposed strain along the Z-axis. The number of elements and the exact detail of the node locations were varied from case to case, to gain experience in the effect of these changes on the solution; usually about 150 elements was the maximum used. The specified restrictions, which were only on particular node movements, provided for a given change in specimen dimensions (e.g., 40% extension). By selecting a particular isochrone for K_1, the strain rate was then set (e.g., the 1.0-min isochrone would then specify a specimen extension rate of 40%/min). As mentioned, K_2 was set at 0.5 at all times and strains, and K_3 and K_4 were set at zero. Since the K_3 isochrones were obtained from constant strain rate uniaxial data, the implicit assumption was made that all elements of a specimen were undergoing constant strain rate deformation (but at different rates) during the constant strain rate extension (or compression) of the specimen.

Within these limits, the computer program then processed the data in this manner: for the (so far undeformed) specimen, for each element in turn, the "centroid" was located by averaging the X- and Y-coordinates of the four nodes; the centroid and each adjacent pair of nodes then subdivided each quadrilateral element into four triangles. From the displacements of the four nodes, the principal strain, E_{11}, was calculated and used to obtain values for K_1, K_2, K_3, and K_4 by interpolation in the input tables. These values were used with the geometric information to calculate triangular "element stiffnesses" which were summed into quadrilateral element stiffnesses. As the elements were processed, these element stiffnesses were further summed into a set of structural stiffness equations, containing as unknowns the X- and Y-displacements of all the nodes that had not been fixed in the input.

Finally these simultaneous equations were solved by a least-squares procedure which yielded a set of displacements (and from them a set of calculated stresses) that was consistent with the imposed deformation and the particular set of element parameters (i.e., K_1 to K_4 for each quadrilateral element) that had been found by the tabular interpolation. If this had been a small strain problem, the calculation would then be over. That is, on this first set of solutions, K_1, etc., would have been obtained at $E_{11} = 0$, so the time-dependent shear modulus alone would have been used to calculate the stress and strain pattern. (Remember that $K_2 = 0.5$ and $K_3 = K_4 = 0$ were set up by our input.) Since this is a large strain problem, we must consider that the shear modulus is not appropriate when $E_{11} > 0$; instead the K_1 value must be found for E_{11} for each element. Consequently, the program now recalculated the centroid location and the E_{11} value for each now-deformed element and repeated the tabular interpolation of material parameters and element stiffness calculations and summations, eventually re-solving the simultaneous stiffness equations to get a new set of X- and Y-displacements.

Obviously, if the new set was essentially the same as the previous set, there would be no need for further iterations of this procedure and the solution would be at hand. It can be seen from eq. (6) that the K_1 value at zero strain is smaller than the appropriate value at any finite strain. Hence the calculated nodal displacements after the first iteration would be too large, particularly for highly deformed elements. To counteract this, a "creeping up" procedure had been built into the program. This proceeded by multiplying the calculated displacement of each node (from its position at the previous iteration) by a "relaxation factor" (a number between zero and one) so as to reduce the magnitude of the shift of the nodes and thus reduce the magnitude of the jump in K_1 values from iteration to iteration. These relaxation factors were specified as part of the input, as was the maximum number of iterations permitted and the convergence criterion. The latter was tested after each iteration (after applying the relaxation factor) by averaging the displacements of all the nodes on the latest iteration and dividing this by the average overall displacement of all the nodes from the original undeformed positions. When the latest iteration gave a fractional average displacement less than the convergence criterion (or if the maximum number of iterations had been reached), the program exited from the iteration process and calculated the final set of stresses and strains. In many cases, the convergence criterion used was 1%, since it was likely that measurement errors of strain on the ring test samples and the model-joint test samples would be at least this great.

The output of the computer program could be quite voluminous. For each iteration, the location of each node is given, so it is possible to trace the response of the specimen shape to the stepwise imposition of the specified restrictions (e.g., the imposed elongation) and to plot the final shape of the joint seal, including detail of the distribution of displacements. For each element, the three-dimensional components of the stress at the centroid and of the strain are given, as well as the maximum and minimum values of the stress and strain ellipsoids, the direction of the stress maximum, and the strain energy of the element. By summing the stress components over a properly chosen group of elements, the force needed to maintain the imposed deformation is obtained. From the calculated stresses at the element centroids, the distribution pattern of the stresses may be inferred. In favorable cases, the pattern is smooth enough to permit the drawing of contour lines of constant local maximum tensile stress, here termed isodynics. Distribution patterns may also be inferred of the stress components, as well as of the angle of local maximum stress, of the maximum local strain and strain components, and of the strain energy density.

Testing in all detail of these computer predictions is not practical. The measured shape can be compared to prediction, as can the total force needed to deform the joint seal. Such comparisons will be made for some model joints in the next article.[4] In principle, at least, "frozen stress" photoelastic techniques[21] could be used to test the predicted stress distributions. This would require selection of a clear photoelastic resin having essentially the same K_1 versus large strain tensor properties as the sealant material, a much more stringent requirement than simply matching the zero-strain shear modulus and restricting study to the "effectively linear behavior" regions of both model resin and prototype material.[22] The basic computer program has indeed been used to predict such photoelastic patterns within the rocket propellant industry.

GLOSSARY OF SYMBOLS

C_1,C_2 = parameters of Mooney-Rivlin phenomenologic theory of elastic behavior[18]

D_i = inside diameter of ring sample

D_0 = outside diameter of ring sample

d_0 = initial depth of fill of a rectangular butt-joint seal

$E(t)$ = tensile stress–relaxation modulus = σ/ϵ in a simple tensile stress–relaxation experiment at constant ϵ

E_{ij} = large strain tensor[13]

E_{11} = principal component of the large strain tensor $E_{ij} = 0.5\ (1 - \lambda_1^{-2})$ in uniaxial extension

e_v = measure of volume change = $0.5\ (1 - J_3^{-2})$[9]

$F(t)$ = constant strain rate tensile modulus = σ/ϵ in a constant rate of extension stress–strain test starting at zero strain[5]

$f(t)$ = generalized time-dependent modulus

$G(t)$ = time-dependent shear modulus

$g(\epsilon)$ = $\Phi(\epsilon)/\epsilon$; this is the reciprocal of Smith's $g(\epsilon)$[5]

h = amount of "curve-in" or neck-down of a rectangular butt-joint seal on stretching

J_3 = relative volume = V/V_0

K_1 = strain- and time-dependent material parameter which reduces to the time-dependent shear modulus at infinitesimal strain[9]

K_2 = strain-dependent material parameter which expresses volume change on deformation and, like the generalized Poisson ratio, is 0.5 for isovolumetric deformation[9]

K_3 = strain-dependent material parameter which expresses strain-induced anisotropy; zero at infinitesimal strain[11]

K_4 = strain-dependent material parameter which is needed for full three-dimensional analysis; zero at infinitesimal strain[11,12]

L_0 = initial sample length

t	= time since application of force
V	= sample volume
V_0	= volume of undeformed sample
ϵ	= engineering strain, deformation/undeformed length $= \lambda - 1$
ϵ_{lat}	= transverse strain, transverse deformation/undeformed width $= 1 - \lambda_{lat}$
λ	= extension ratio, deformed length/undeformed length
λ_{lat}	= transverse dimension ratio, deformed width/undeformed width
ν	= generalized Poisson ratio[17]
ν_0	= Poisson's ratio for small tensile strain $= \epsilon_{lat}/\epsilon$
σ	= nominal stress, applied force/area of undeformed specimen
σ^*	= true stress, net force/area of deformed specimen
$\Phi(\epsilon)$	= generalized function of extension, empirical measure of strain
ϕ	= relative volume dilatation $= J_3 - 1$

References

1. J. R. Panek and C. H. Wells, *Bulk Sealants Used in Building Joints*, CSI Monograph 10M1, Washington, D.C., April 1969.
2. E. Tons, *A Theoretical Approach to Design of a Road Joint Seal*, Highway Research Board, Bulletin 229, January 1959.
3. J. P. Cook, Ph.D. Thesis, Rensselaer Polytechnic Institute (1963).
4. E. H. Catsiff, R. F. Hoffman, and R. T. Kowalewski, *J. Appl. Polym. Sci.*, **14**, No. 5 (1969).
5. T. L. Smith, *Trans. Soc. Rheology*, **6**, 61 (1962).
6. A. V. Tobolsky and J. R. McLoughlin, *J. Polym. Sci.*, **8**, 543 (1952).
7. J. D. Ferry, *J. Amer. Chem. Soc.*, **72**, 3746 (1950).
8. R. D. Andrews, Jr., N. Hofman-Bang, and A. V. Tobolsky, Chap. II in *Relaxation of Stress and Permanent Set in Rubber-like Polymers*, (Ph.D. Dissertation of R. D. Andrews, Jr., Princeton Univ., 1948, pp. 7–13).
9. L. R. Herrmann, Bulletin of the 4th Meeting, ICRPG, Working Group on Mechanical Behavior, Vol. 1, Nov. 1965, p. 405.
10. F. E. Peterson, D. M., Campbell and L. R. Herrmann, Bulletin of the 5th Meeting, ICRPG, Working Group on Mechanical Behavior, Vol. 1, Nov. 1966, p. 421.
11. L. R. Herrmann, private communication.
12. G. P. Anderson, private communication.
13. A. E. Green and W. Zerna, *Theoretical Elasticity*, Clarendon Press, Oxford, 1954.
14. R. S. Rivlin and D. W. Saunders, *Phil. Trans. Roy. Soc. A*, **243**, 251 (1951).
15. A. N. Gent and R. S. Rivlin, *Proc. Phys. Soc.*, **B65**, 118, 487, 645 (1952).
16. L. R. G. Treloar, *Proc. Phys. Soc.*, **60**, 135 (1948).
17. P. J. Blatz and W. L. Ko, *Trans. Soc. Rheology*, **6**, 223 (1962).
18. L. R. G. Treloar, *The Physics of Rubber Elasticity*, Clarendon Press, Oxford, 1958.
19. E. B. Becker and J. J. Brisbane, Rohm & Haas Co. Special Report No. S-76, *Application of the Finite Element Method to Stress Analysis of Solid Propellant Rocke Grains*, Columbus, Ohio, 1965.
20. L. R. Herrmann, *A.I.A.A. J.*, **3**, 1896 (1965).
21. D. Post, Chap. IV in *Manual on Experimental Stress Analysis*, 2nd ed., Soc. for Exptl. Stress Analysis, Westport, Conn., 1965.
22. E. W. Kiesing and J. T. Pindera, *Exptl. Mechanics*, **9**, 337 (1969).

Received October 24, 1969
Revised January 16, 1970